minerals

MDPI

Article

$Zn(NH_3)_2Cl_2$, a Mineral-like Anthropogenic Phase with Ammine Complexes from the Burned Dumps of the Chelyabinsk Coal Basin, South Urals, Russia: Crystal Structure, Spectroscopy and Thermal Evolution

Andrey A. Zolotarev [1,*], Margarita S. Avdontceva [1], Rezeda M. Sheveleva [1], Igor V. Pekov [2], Natalia S. Vlasenko [3], Vladimir N. Bocharov [3], Maria G. Krzhizhanovskaya [1], Anatoly A. Zolotarev [1], Mikhail A. Rassomakhin [4] and Sergey V. Krivovichev [1,5]

1 Institute of Earth Sciences, St. Petersburg State University, 199034 St. Petersburg, Russia; m.avdontceva@spbu.ru (M.S.A.); rezeda_marsovna@inbox.ru (R.M.S.); mariya.krzhizhanovskaya@spbu.ru (M.G.K.); a.a.zolotarev@spbu.ru (A.A.Z.); s.krivovichev@spbu.ru (S.V.K.)
2 Faculty of Geology, Moscow State University, 119991 Moscow, Russia; igorpekov@mail.ru
3 Centre for Geo-Environmental Research and Modelling, St. Petersburg State University, 199034 St. Petersburg, Russia; n.vlasenko@spbu.ru (N.S.V.); bocharov@molsp.phys.spbu.ru (V.N.B.)
4 South Urals Federal Research Center of Mineralogy and Geoecology of UB RAS, 456317 Miass, Russia; miha_rassomahin@mail.ru
5 Nanomaterials Research Centre, Kola Science Center, Russian Academy of Sciences, 184209 Apatity, Russia
* Correspondence: a.zolotarev@spbu.ru

check for updates

Citation: Zolotarev, A.A.; Avdontceva, M.S.; Sheveleva, R.M.; Pekov, I.V.; Vlasenko, N.S.; Bocharov, V.N.; Krzhizhanovskaya, M.G.; Zolotarev, A.A.; Rassomakhin, M.A.; Krivovichev, S.V. $Zn(NH_3)_2Cl_2$, a Mineral-like Anthropogenic Phase with Ammine Complexes from the Burned Dumps of the Chelyabinsk Coal Basin, South Urals, Russia: Crystal Structure, Spectroscopy and Thermal Evolution. *Minerals* **2023**, *13*, 1109. https://doi.org/10.3390/min13081109

Academic Editors: Mariola Kadziolka-Gawel and Mateusz Dulski

Received: 10 July 2023
Revised: 10 August 2023
Accepted: 18 August 2023
Published: 21 August 2023

Abstract: The mineral-like anthropogenic phase $Zn(NH_3)_2Cl_2$, with ammine (NH_3^0) complexes from the burned dumps of the Chelyabinsk coal basin (South Urals, Russia), has been investigated using single-crystal and high-temperature powder X-ray diffraction, and Raman and infrared (IR) spectroscopy. The anthropogenic $Zn(NH_3)_2Cl_2$ is orthorhombic, *Imma*, a = 7.7399(6), b = 8.0551(5), c = 8.4767(8) Å, V = 528.49(7) Å^3, R_1 = 0.0388 at −73 °C. Its crystal structure is based upon isolated ZnN_2Cl_2 tetrahedra connected by hydrogen bonds (between NH_3 groups and Cl atoms) into a three-dimensional network. Upon heating, the $Zn(NH_3)_2Cl_2$ phase is stable up to about 150 °C, which is in good agreement with the data on the temperature of its formation. The crystal structure of $Zn(NH_3)Cl_2$ expands anisotropically with the strongest thermal expansion observed along the a axis. The thermal expansion of the structure is controlled by the changes in the hydrogen bonding system. The Raman and IR spectroscopic characteristics of this phase are close to those of the mineral ammineite, $CuCl_2(NH_3)_2$. The studied anthropogenic phase, formed in the unique conditions of burned coal dumps, is identical to the synthetic $Zn(NH_3)_2Cl_2$.

Keywords: $Zn(NH_3)_2Cl_2$; anthropogenic mineral-like phase; burned coal dumps; Chelyabinsk coal basin; crystal structure; Raman spectroscopy; infrared spectroscopy; thermal behavior

1. Introduction

$Zn(NH_3)_2Cl_2$, an anthropogenic mineral-like phase, was found by Chesnokov and co-authors in the burned coal dumps of the Chelyabinsk coal basin (ChCB) in the South Urals, Russia in 1984 [1]. The Chelyabinsk burned coal dumps are well-known for their anthropogenic mineral-like phases. More than 240 different compounds have been found in this region and about 50 of them were unique at the time of their first description. Eight phases found in the Chelyabinsk dumps were approved as new mineral species, with the ChCB as a type locality [2].

At least sixteen different ammonium-bearing phases from the ChCB are of special interest as they are formed through the contact of burning coal with organic matter at elevated temperatures. Their formation involves crystallization from gases, the phases are

formed during the so-called "pseudofumarole" stage or as a result of supergene process, and they have much in common with the fumarolic ammonium minerals and similar minerals formed by the reactions of mineral components with organic substance, for example, guano [3–5]. At the same time, only one phase containing ammine (NH_3^0) complexes, $Zn(NH_3)_2Cl_2$, has been described from the ChCB burned dumps. This work is devoted to the crystal chemical features of this phase found at the ChCB.

In general, minerals containing NH_3^0 complexes are very specific and extremely rare. Only five such compounds are IMA-approved mineral species which have completely natural origin. They were all described from the Pabellon de Pica guano deposit near Chanabaya, Iquique Province, Tarapacá, Chile, namely ammineite, $CuCl_2(NH_3)_2$ [6]; chanabayaite, $Cu_2Cl(N_3C_2H_2)_2(NH_3,Cl,H_2O,\square)_4$ [7]; triazolite, $NaCu_2(N_3C_2H_2)_2(NH_3)_2Cl_3{\cdot}4H_2O$ [8]; shilovite, $Cu(NH_3)_4(NO_3)_2$ [9]; and joanneumite, $Cu(C_3N_3O_3H_2)_2(NH_3)_2$ [10].

The synthetic compound $Zn(NH_3)_2Cl_2$ (zinc diammine chloride, or diamminedichlorozinc) is well known in the chemistry of complex compounds [11] and belongs to the class of diamminechlorides (chlorides containing two NH_3 complexes) of various divalent metals with the general formula $M^{2+}(NH_3)_2Cl_2$, where M^{2+} = Cu, Zn, Mg, Fe, Co, Ni, Cd, Hg, Ca and Pt. In nature, except for ammineite, $CuCl_2(NH_3)_2$ [6], no such compounds have been described so far. Some synthetic metal chlorides with ammine complexes have applications in technologies and medicine: for example, the cis-$[PtCl_2(NH_3)_2]$ complex (Cisplatin) is an important anticancer drug [12] and the compound $Mg(NH_3)_6Cl_2$ is considered as a solid matrix for hydrogen storage [13].

The purpose of this work is a detailed crystal chemical description of a mineral-like anthropogenic $Zn(NH_3)_2Cl_2$ from the ChCB burned dumps, including the determination of its crystal structure, spectroscopic studies and the correlation of the obtained results with the data known for its synthetic analogue. One of the aims of the current study is to investigate the thermal evolution of anthropogenic $Zn(NH_3)_2Cl_2$ by means of in situ single-crystal and powder X-ray diffraction studies at different temperatures. Such an investigation is of interest since $Zn(NH_3)_2Cl_2$ was found in discharged air–zinc batteries and may also be a byproduct of hydrocracking of heavy oil fractions (see [14,15] and references therein). The thermal stability and thermodynamic characteristics of synthetic $Zn(NH_3)_2Cl_2$ have been well studied (see [15] and references therein). However, data from in situ X-ray diffraction studies at different temperatures are absent in the literature and would complement the characterization of the thermal evolution of $Zn(NH_3)_2Cl_2$, taking into account its formation under the conditions of the burning dumps of the ChCB.

2. Materials and Methods

2.1. Occurrence

The studied sample of the mineral-like anthropogenic $Zn(NH_3)_2Cl_2$ phase was taken from the collection of Prof. Boris V. Chesnokov (1928–2005), which is deposited in the Natural Science Museum of the Ilmen State Reserve (Miass, Russia) under catalogue number 099-10. It was described by Chesnokov and co-authors as "amminite" from a burning coal heap located near the town of Gornyak at the northern border of the city Kopeisk. This compound was found among the alteration products of a zinc plate placed in the near-surface part of burning coal-bearing material for nine days. It forms colorless or brownish crystals (Figure 1) closely associated with ZnO (anthropogenic analogue of zincite) and $Zn_5Cl_2(OH)_8$ ("chlorozincite"). According to Chesnokov and co-authors, the formation of $Zn(NH_3)_2Cl_2$ occurred at temperatures lower than 200 °C as a result of the interaction between Zn or ZnO with hot gas enriched by chlorine and nitrogen compounds [1].

2.2. Chemical Composition

Several crystals of $Zn(NH_3)_2Cl_2$ were mounted in epoxy blocks and polished without exposure to water. The samples were coated with a 10 nm conductive carbon layer for scanning electron microscopy (SEM) studies. Quantitative elemental analysis was carried out using a Hitachi S-3400N scanning electron microscope with an Oxford Instruments Energy

Dispersive Spectrometer X-Max (20 kV and 1.7 nA, the working distance is 10 mm). The energy-dispersive spectra were processed automatically using the AzTec Energy software package using the TrueQ technique. The X-ray acquisition time was 30 s in spot mode. Quantification of elemental compositions was conducted using standard samples of natural and synthetic compounds: Zn for Zn, NaCl for Cl and BN for N. Since nitrogen was only determined semi-quantitatively, its amount was calculated based on structural data, as well as the amount of hydrogen.

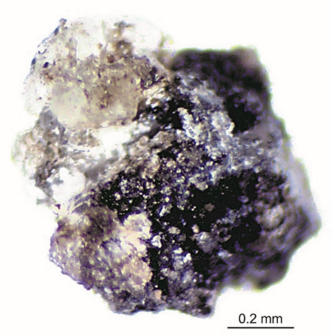

Figure 1. The colorless and brownish crystals of $Zn(NH_3)_2Cl_2$ from the burned dump of the ChCB.

2.3. Raman Spectroscopy

The Raman spectrum of $Zn(NH_3)_2Cl_2$ was obtained using a Horiba Jobin-Yvon LabRam HR 800 system at room temperature in the range of 70–4000 cm^{-1} using a solid state laser (λ = 532 nm, power on the sample 8 mW) and 50× objective. The equipment was calibrated according to a silicon standard. The sample was oriented randomly. The data accumulation time took from 2 to 10 s. The obtained spectrum was visualized in OriginPro 2018 SR1 b9.5.1.195.

2.4. Infrared Spectroscopy

The infrared (IR) spectrum of $Zn(NH_3)_2Cl_2$ was obtained using a Bruker Vertex 70 FTIR spectrometer with the KBr pellet method (200 mg of KBr and 2 mg of the sample) in the range of 4000–370 cm^{-1}.

2.5. Single-Crystal X-ray Diffraction

Single-crystal X-ray diffraction (SCXRD) studies of $Zn(NH_3)_2Cl_2$ were performed using a Rigaku XtaLAB Synergy-S diffractometer (MoKα radiation, 50 kV and 1.0 mA, frame widths 0.5° in ω and 10 s counting time for each frame) with high-stability microfocus X-ray source PhotonJet-S and a high-speed hybrid photon counting detector HyPix-6000HE. The single-crystal X-ray diffraction studies in air were kept in situ at the following temperatures: −173 °C, −123 °C, −73 °C, −23 °C, 27 °C, 77 °C and 127 °C (at 127 °C, the crystal lost crystallinity within a relatively short time; for this reason, SCXRD data for this temperature were not obtained) using the Oxford Cryosystems Cryostream. SCXRD data were collected at different temperatures without changing the orientation of the crystal. The main coefficients of the thermal expansion tensor were determined using the TTT program package [16].

The CrysAlisPro software was used for data processing [17]. An absorption correction was introduced using the SCALE3 ABSPACK algorithm. The structures have been solved and refined using ShelX program package [18] within the Olex2 shell [19]. Crystal data, data collection information and structure refinement details at −73 °C (at this temperature, the refinement parameters were the best, so this is the reason why we have provided all the main structural data for this temperature) are given in Table 1; atom coordinates and displacement parameters are shown in Tables 2 and 3 and selected interatomic distances and angles are presented in Tables 4 and S1, respectively. H-atoms were derived from an analysis of the Fourier difference electron-density maps and refined freely in an isotropic approximation. The parameters of the hydrogen bonds of $Zn(NH_3)_2Cl_2$ at different temperatures are given

in Table 5. The unit-cell parameters of $Zn(NH_3)_2Cl_2$ at different temperatures are shown in Table 6. Vesta software was used to visualize the structural data [20].

Table 1. Crystal data and structure refinement of $Zn(NH_3)_2Cl_2$ at −73 °C.

Crystal System	Orthorhombic
Space group	*Imma*
a, Å	7.7399(6)
b, Å	8.0551(5)
c, Å	8.4767(8)
Volume, Å^3	528.49(7)
Z	4
$D_{c_{alc}}$, g/cm^{-3}	2.141
μ, mm^{-1}	5.494
F(000)	336.0
Crystal size, mm	0.16 × 0.12 × 0.08
Radiation	Mo*Kα* (λ = 0.71073)
2Θ range for data collection, °	6.978 to 67.308
Index ranges	$-9 \leq h \leq 10$, $-8 \leq k \leq 12$, $-12 \leq l \leq 10$
Reflections collected	1668
Independent reflections	497 [R_{int} = 0.0420, R_{sigma} = 0.0425]
Data/restraints/parameters	497/0/24
Goodness-of-fit on F^2	1.018
Final *R* indexes [$I \geq 2\sigma$ (*I*)]	R_1 = 0.0388, wR_2 = 0.0994
Final *R* indexes [all data]	R_1 = 0.0486, wR_2 = 0.1050
Largest diff. peak/hole/e Å^{-3}	1.01/−0.63

Table 2. Atomic coordinates and equivalent isotropic displacement parameters (Å^2) of $Zn(NH_3)_2Cl_2$ at −73 °C.

Atom	*x*	*y*	*z*	U(eq)
Zn1	$\frac{1}{2}$	$\frac{1}{4}$	0.61307(7)	0.0237(2)
Cl1	$\frac{1}{2}$	0.47901(11)	0.76901(12)	0.0271(3)
N1	0.2843(5)	$\frac{1}{4}$	0.4814(5)	0.0289(7)
H1A	0.270(7)	0.322(6)	0.4140(5)	0.056(14)
H1B	0.189(10)	$\frac{1}{4}$	0.526(9)	0.060(20)

Table 3. Anisotropic displacement parameters (Å^2) of $Zn(NH_3)_2Cl_2$ at −73 °C.

Atom	U_{11}	U_{22}	U_{33}	U_{23}	U_{13}	U_{12}
Zn1	0.0245(4)	0.0247(3)	0.0219(4)	0	0	0
Cl1	0.0282(5)	0.0249(4)	0.0281(5)	−0.0046(3)	0	0
N1	0.0272(17)	0.0361(17)	0.0234(17)	0	−0.0014(14)	0

Table 4. Selected bond lengths (Å) and angles (°) of $Zn(NH_3)_2Cl_2$ at −73 °C.

Atom	Atom	Length	Atom	Atom	Atom	Angle
Zn1	Cl1	2.2694(10)	Cl1	Zn1	Cl1 [1]	108.75(5)
Zn1	Cl1 [1]	2.2695(10)	N1	Zn1	Cl1	108.89(6)
Zn1	N1	2.008(4)	N1 [1]	Zn1	Cl1 [1]	108.89(6)
Zn1	N1 [1]	2.008(4)	N1	Zn1	Cl1 [1]	108.89(6)
			N1 [1]	Zn1	Cl1	108.89(6)
			N1	Zn1	N1 [1]	112.5(2)

[1] 1 − X, 1/2 − Y, +Z.

Table 5. Hydrogen bonds of $Zn(NH_3)_2Cl_2$ at different temperatures.

D-H (Å)	H...A (Å)	D...A (Å)	<(DHA)°	D-H...A
		−173 °C		
0.74(5)	2.83(6)	3.458(3)	143(6)	N1-H1A...Cl1 [1]
0.74(5)	2.99(6)	3.549(3)	134(6)	N1-H1A...Cl1 [2]
0.91(8)	2.83(6)	3.548(4)	136.9(19)	N1-H1B...Cl1 [3]
0.91(8)	2.83(6)	3.548(4)	136.9(19)	N1-H1B...Cl1 [4]
		−123 °C		
0.77(7)	2.81(7)	3.464(3)	144(7)	N1-H1A...Cl1 [1]
0.77(7)	3.00(8)	3.564(3)	132(7)	N1-H1A...Cl1 [2]
0.82(10)	2.90(8)	3.559(4)	138(2)	N1-H1B...Cl1 [3]
0.82(10)	2.90(8)	3.559(4)	138(2)	N1-H1B...Cl1 [4]
		−73 °C		
0.83(5)	2.85(5)	3.472(3)	133(5)	N1-H1A...Cl1 [1]
0.83(5)	2.90(5)	3.585(3)	141(5)	N1-H1A...Cl1 [2]
0.83(8)	2.93(7)	3.567(4)	136(3)	N1-H1B...Cl1 [3]
0.83(8)	2.93(7)	3.567(4)	136(3)	N1-H1B...Cl1 [4]
		−23 °C		
0.84(5)	2.78(5)	3.486(4)	142(5)	N1-H1A...Cl1 [1]
0.84(5)	2.99(5)	3.598(3)	131(5)	N1-H1A...Cl1 [2]
0.81(10)	2.95(8)	3.573(4)	135(3)	N1-H1B...Cl1 [3]
0.81(10)	2.95(8)	3.573(4)	135(3)	N1-H1B...Cl1 [4]
		27 °C		
0.79(6)	2.83(7)	3.493(4)	142(6)	N1-H1A...Cl1 [1]
0.79(6)	3.03(7)	3.615(4)	132(6)	N1-H1A...Cl1 [2]
0.77(9)	3.00(7)	3.586(5)	135(4)	N1-H1B...Cl1 [3]
0.77(9)	3.00(7)	3.586(5)	135(4)	N1-H1B...Cl1 [4]
		77 °C		
0.81(7)	2.85(7)	3.502(6)	139(6)	N1-H1A...Cl1 [1]
0.81(7)	3.01(7)	3.634(4)	136(6)	N1-H1A...Cl1 [2]
0.73(14)	3.01(11)	3.594(6)	139(4)	N1-H1B...Cl1 [3]
0.73(14)	3.01(11)	3.594(6)	139(4)	N1-H1B...Cl1 [4]

[1] +X,1 − Y, 1 − Z; [2] 1/2 − X, 1 − Y, − 1/2 + Z; [3] 1/2 − X, +Y, 3/2 − Z; [4] −1/2 + X, 1/2 − Y, 3/2 − Z.

Table 6. The unit-cell parameters (Å) and Volume (Å^3) of $Zn(NH_3)_2Cl_2$ at different temperatures.

	a	*b*	*c*	*V*
		anthropogenic (our data)		
−173 °C	7.6965(8)	8.0158(7)	8.4556(10)	521.66(9)
−123 °C	7.7181(6)	8.0365(5)	8.4696(7)	525.34(7)
−73 °C	7.7399(6)	8.0551(5)	8.4767(8)	528.49(7)
−23 °C	7.7679(7)	8.0769(6)	8.4933(9)	532.87(8)
27 °C	7.7917(9)	8.0974(8)	8.5162(11)	537.31(11)
77 °C	7.8080(9)	8.1187(7)	8.5325(11)	540.88(10)
		synthetic [14]		
−173 °C	7.7077(2)	8.0226(2)	8.4526(3)	522.67(3)

2.6. High-Temperature Powder X-ray Diffraction

The thermal behavior of $Zn(NH_3)_2Cl_2$ was studied in air using an in situ high-temperature powder X-ray diffraction (HTXRD) method, using a Rigaku Ultima IV diffractometer (Cu*Kα* radiation, 40 kV/30 mA, Bragg-Brentano geometry, high-speed DTEX Ultra 1D detector, Pt substrate) with a Rigaku SHT 1500 high-temperature attachment. The

sample was studied in the temperature range 30–250 °C with 10 °C steps (Figure S1). The room-temperature data were loaded into PDXL [21] to check the phase composition. The TOPAS software package [22] was used for the refinement of unit-cell parameters at all temperatures using the Pawley method. The background was modelled using a Chebyshev polynomial approximation of the 9th order. The peak profile was described using the fundamental parameters approach. The main coefficients of the thermal expansion tensor were determined using the TTT program package [16].

2.7. Structural Complexity

The structural complexity of $Zn(NH_3)_2Cl_2$ was calculated using the ToposPro software package [23] for the model with localized hydrogen atoms (our data), as well as for the models without localized hydrogen atoms [24]. The structural complexity calculation approach is based on the amount of Shannon information measured in bits per atom (I_G, bits/atom) and per unit cell ($I_{G,total}$, bits/cell), the method of numerical evaluation of structural complexity was developed by S.V. Krivovichev (see [25,26] and references therein).

3. Results

3.1. Chemical Composition

The empirical formula of $Zn(NH_3)_2Cl_2$ was calculated on the basis of 2 Cl atoms per formula unit; the N and H amounts were calculated using stoichiometry from the structure refinement (Table 7). Unfortunately, the $Zn(NH_3)_2Cl_2$ phase is unstable and apparently partially oxidized, so the analyses were normalized to 100 wt. %. Despite this fact, the analyses show a good agreement with the Zn:Cl~1:2 stoichiometry.

Table 7. Chemical composition of $Zn(NH_3)_2Cl_2$.

Constituent [1]	wt. % [2]	a.p.f.u. [3]
Zn	38.66	1.01
Cl	41.46	2
N_{calc}	16.37	2
H_{calc}	3.51	6
Total	100	

[1] Nitrogen and hydrogen contents were calculated from the crystal structure data; [2] The analyses were normalized to 100 wt. %; [3] Atoms per formula unit.

3.2. Raman Spectroscopy

In general, the spectrum obtained for $Zn(NH_3)_2Cl_2$ has many similarities with the spectrum described for ammineite, $CuCl_2(NH_3)_2$ (see Table S2 for details), which also contains ammine complexes [27]. The most intense modes of the spectrum correspond to the stretching vibrations of the NH_3 groups and Zn-N and Zn-Cl stretching and bending vibrations (Figure 2). The bands at <200 cm^{-1} can be assigned to lattice modes. The intense band at 281 cm^{-1} is probably connected with the symmetric stretching vibrations (ν_s) of zinc-halogen (Zn-Cl), whereas the band at 417 cm^{-1} corresponds to the ν_s Zn-N vibration modes [27,28]. The medium intense bands at 633 cm^{-1} and 682 cm^{-1} are connected with rocking vibration modes of NH_3. The region from 3000 to 3500 cm^{-1} (3255 cm^{-1} (ν_s), 3170 (m), 3332 (m)) can be attributed to the stretching N-H vibration modes [29]. The low-intensity bands at 1333 cm^{-1}, 1457 cm^{-1} and 1594 cm^{-1} can relate to the symmetric (δ_s) and asymmetric (δ_{as}) bending modes of NH_3 [28]. The bands in the ranges 1750–3000 cm^{-1} and also 3500–4000 cm^{-1} are not clearly identified, but it can be assumed that they correspond to spectral artifacts.

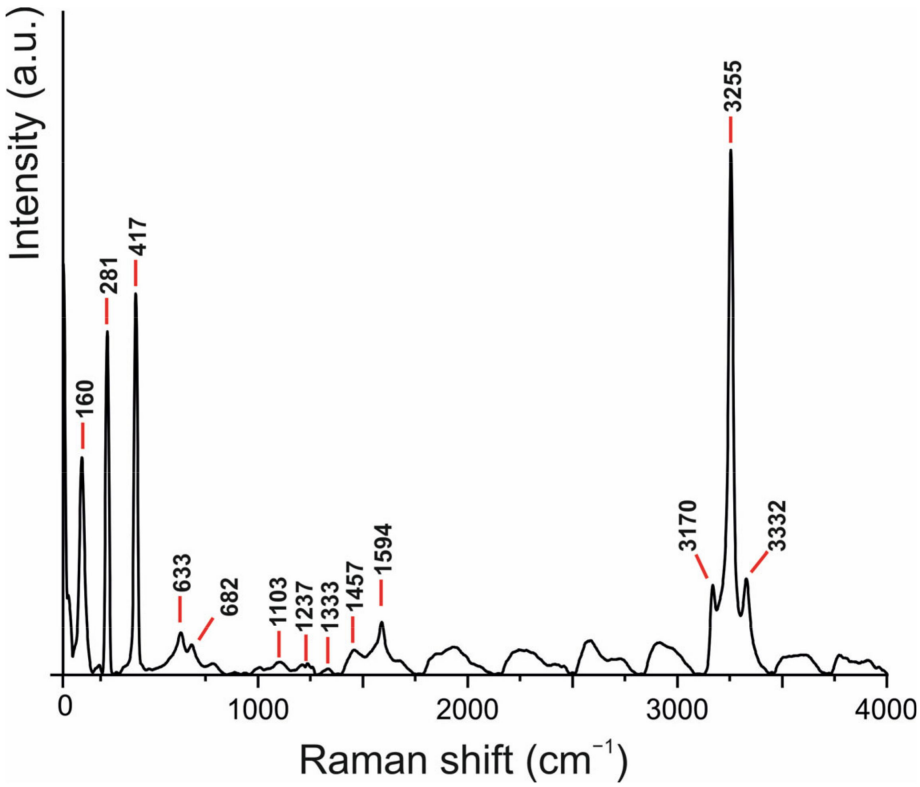

Figure 2. Raman spectrum of $Zn(NH_3)_2Cl_2$.

3.3. Infrared Spectroscopy

The IR spectrum of $Zn(NH_3)_2Cl_2$ (Figure 3) is close to the spectrum of "amminite", $Zn(NH_3)_2Cl_2$, from Kopeisk earlier reported by Chukanov [30]. Most intense bands of $Zn(NH_3)_2Cl_2$ are assigned to the vibrations of the NH_3-groups. Thus, according to Bojar et al. (see [6] and references therein), the bands in the range 3400–3000 cm^{-1} (3328, 3192, 3161 and their shoulders) correspond to antisymmetric and symmetric (NH_3) stretching vibrations. We assume that the band at 3497 cm^{-1} can also be assigned to antisymmetric and symmetric (NH_3) stretching modes. The degenerate bending vibration of δ_d-(NH_3) has a wavenumber of 1617 cm^{-1}. The symmetric deformation of δ_s-(NH_3) appears at 1247 cm^{-1}. The intense band at 1404 cm^{-1} can also be assigned to N-H vibrations (it may also probably be a trace of an ammonium salt impurity [6]). Libration vibrations of ϱ_r-(NH_3) form the triplet with the wavenumbers 684, 642 and 622 cm^{-1} at the IR spectrum of $Zn(NH_3)_2Cl_2$. The weak band at 478 cm^{-1} can be assigned to the Zn-N antisymmetric deformations, and the bands at 417 and 391 cm^{-1} correspond to lattice modes. The bands at 2364 and 2339 cm^{-1} probably correspond to uncompensated atmospheric CO_2 (as well as the "ripples" in the range 1600–1550 cm^{-1} corresponding to atmospheric water). The band at 1124 cm^{-1} probably belongs to an impurity (we can assume that the impurity is a Zn sulphate phase, e.g., goslarite, $ZnSO_4{\cdot}7H_2O$, which is a common supergene zinc sulphate and the most intense band in its IR spectrum demonstrates maximum at 1125 cm^{-1} [30]). The IR spectrum of $Zn(NH_3)_2Cl_2$ is similar to that of ammineite, $CuCl_2(NH_3)_2$ [6,30]. The main NH_3-bands in similar positions were also recently described for $Co(NH_3)_6Cl_3$ by Wang et al. [31]. Noteworthy, the spectra of both "amminite", $Zn(NH_3)_2Cl_2$, (reported by Chukanov) and ammineite, $CuCl_2(NH_3)_2$, do not contain bands in the region 1200–1100 cm^{-1} [6,30].

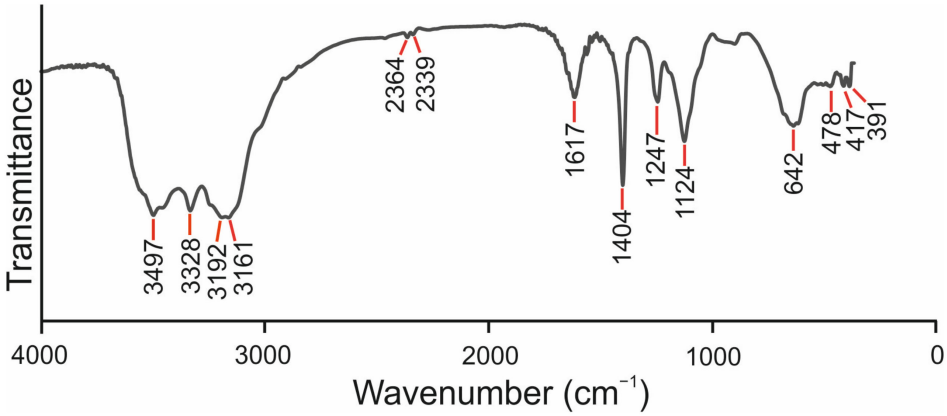

Figure 3. Infrared spectrum of $Zn(NH_3)_2Cl_2$.

3.4. Single-Crystal X-ray Diffraction

The refinement of the crystal structure of anthropogenic $Zn(NH_3)_2Cl_2$ from the ChCB burned dumps demonstrated that this phase is identical to the synthetic compound of the same composition. The anthropogenic $Zn(NH_3)_2Cl_2$ phase is orthorhombic, a = 7.7399(6), b = 8.0551(5), c = 8.4767(8) Å and V = 528.49(7) Å^3 at −73 °C. The structure was refined in the *Imma* space group to R_1 = 0.0388 at −73 °C. For the synthetic compound $Zn(NH_3)_2Cl_2$, the first structural data were obtained in 1936 [32] and the first structural model in 1981 [24], which, however, did not include hydrogen positions. Only relatively recently the crystal structure of the synthetic compound $Zn(NH_3)_2Cl_2$ was refined at −173 °C with localization of hydrogen atoms (*Imma*, a = 7.7077(2), b = 8.0226(2), c = 8.4526(3) Å and V = 522.67(3) Å^3, R_1 = 0.015 at −173 °C) [14].

The crystal structure of $Zn(NH_3)_2Cl_2$ is based upon isolated ZnN_2Cl_2 tetrahedra (Figure 4) connected by hydrogen bonds (between NH_3 groups and Cl atoms) into a three-dimensional network (Figures 5 and 6). The positions of hydrogen atoms localized by our refinement are generally consistent with the model proposed by Ivšić et al. [14]. The parameters of the hydrogen bonds are given in Table 5 and shown in Figures 5 and 6. The Zn-Cl bond length is 2.269 Å and the Zn-N bond length is 2.008 Å (for −73 °C). The SCXRD experiments at different temperatures (from −173 to 127 °C in 50 °C increments) indicated that, at 127 °C, the crystal lost its crystallinity. An analysis of the data shows that, with the increasing temperature, there is a consistent increase in the unit-cell parameters and volume (Table 6).

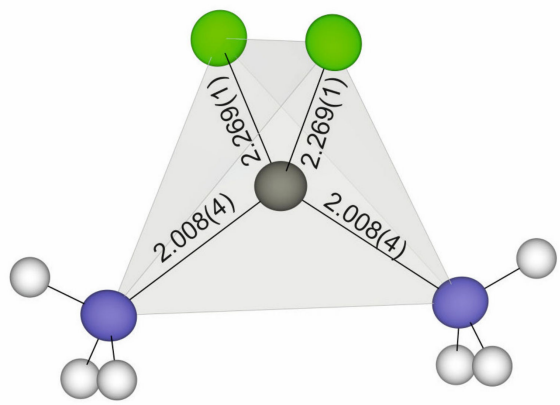

Figure 4. The tetrahedra ZnN_2Cl_2 with bond lengths (Å) indicated for −73 °C. Legend: Zn is shown as gray ellipsoids (displacement ellipsoids, probability 50%), N as blue and Cl as green. Hydrogen atoms are shown as white balls.

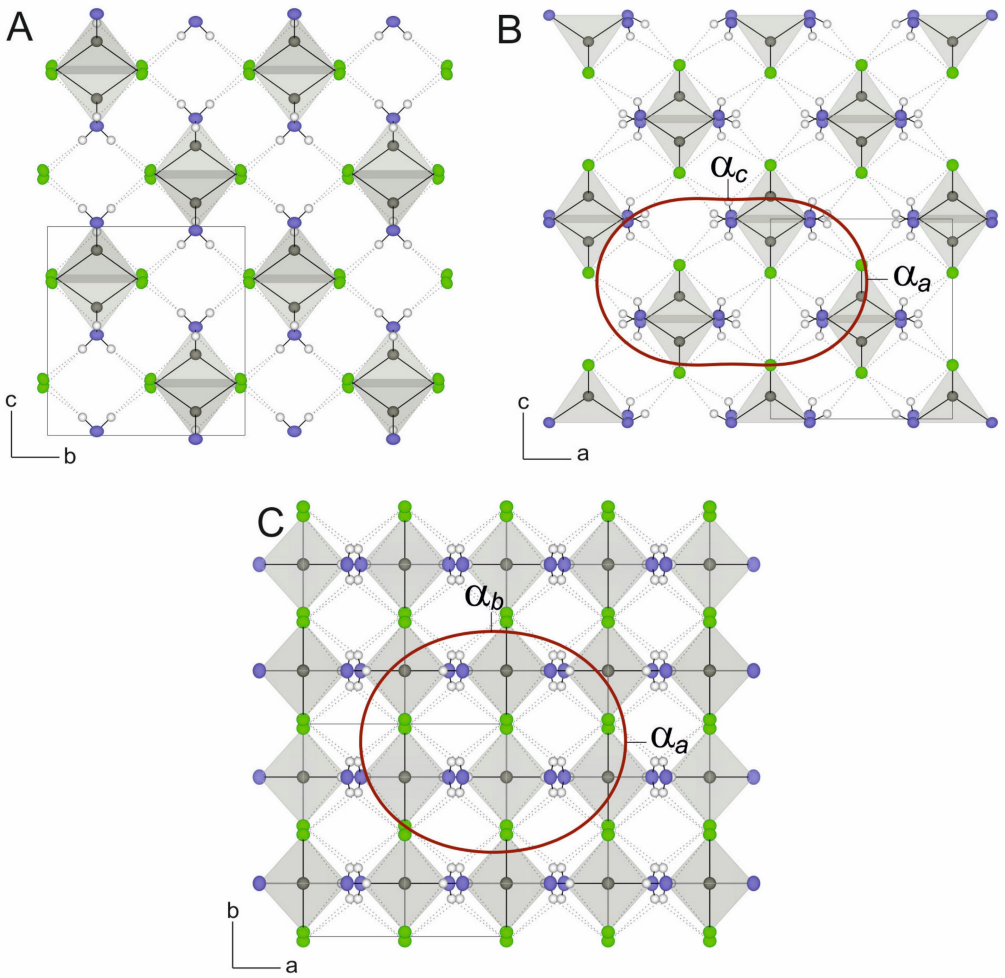

Figure 5. The crystal structure of $Zn(NH_3)_2Cl_2$ and the orientation of the section of the figure of thermal expansion coefficients (red) in the plane (relative to the shown projections): projection on the plane *bc* (**A**), on the plane *ac* (**B**) and on the plane *ab* (**C**). The unit cell is highlighted by the solid black line. Hydrogen bonds are shown with a dotted line. The legend is as in Figure 4.

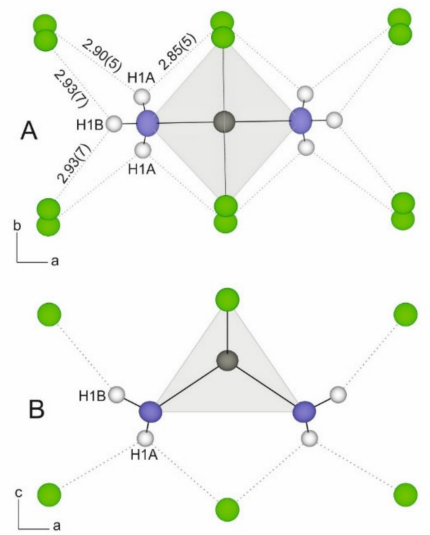

Figure 6. Fragment of the crystal structure of $Zn(NH_3)_2Cl_2$: projection on the plane *ab* (**A**) and on the plane *ac* (**B**). The dotted line shows the hydrogen bonds (the bond lengths Cl...H (Å) are given for temperature −73 °C). The legend is as in Figure 4.

3.5. High-Temperature Powder X-ray Diffraction

The temperature dependencies of the unit-cell parameters are shown in Figure 7. The values obtained from the powder data are shown together with the data from the single crystal experiments at different temperatures. As can be seen from Figure 7, they are in a good agreement. According to the HTXRD experiments, the $Zn(NH_3)Cl_2$ phase is stable up to about 150 °C (Figure S1). At the same time, as per the SCXRD data, the phase begins to lose its crystallinity at 127 °C. It is worth noting that, according to the literature, the synthetic $Zn(NH_3)Cl_2$ phase is stable upon heating up to 190 °C [15]. The difference can probably be explained by the different heating rates and exposure times used in the different methods.

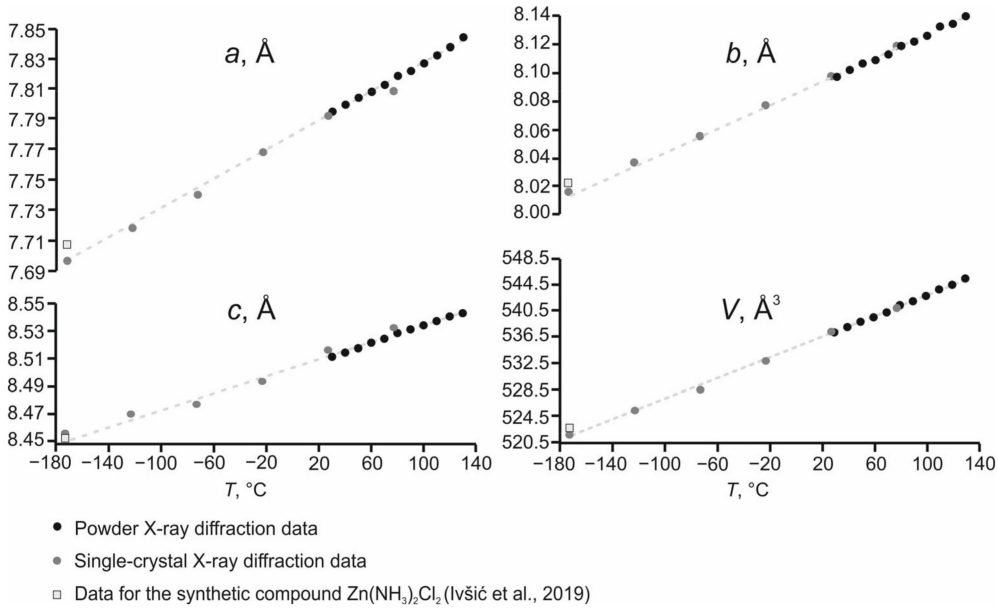

Figure 7. Temperature dependencies of the unit-cell parameters of $Zn(NH_3)_2Cl_2$ (data for synthetic compound according to Ivšić et al. [14]).

The crystal structure of $Zn(NH_3)Cl_2$ expands anisotropically with the strongest thermal expansion observed along the α_a direction (Table 8, Figure 5); the $\alpha_{max}/\alpha_{min}$ value is about 1.64. The parameters for the approximation equations describing the temperature dependences of the unit-cell parameters of $Zn(NH_3)Cl_2$ are given in Table 9.

Table 8. The thermal expansion coefficients of $Zn(NH_3)_2Cl_2$ ($\times 10^6$ °C^{-1}).

T, °C	α_a	α_b	α_c	α_V	$\alpha_V = \alpha_a + \alpha_b + \alpha_c$	$\alpha_{max}/\alpha_{min}$
Based on single-crystal X-ray diffraction data						
−120	59.7(1.8)	51.1(5)	36.5(2.8)	147.3(3.8)	147.32	1.64
−70	59.5(1.8)	51.0(5)	36.4(2.7)	146.9(3.8)	146.89	1.63
−20	59.3(1.8)	50.9(5)	36.4(2.7)	146.5(3.8)	146.56	1.63
30	59.1(1.8)	50.7(5)	36.3(2.7)	146.2(3.7)	146.13	1.63
70	59.0(1.8)	50.6(5)	36.2(2.7)	145.9(3.7)	145.83	1.63
Based on powder X-ray diffraction data						
30	62.9(1.1)	52.2(1)	38.2(5)	153.3(1.8)	153.3	1.65
70	62.7(1.1)	52.1(1)	38.1(5)	152.9(1.7)	152.9	1.65
100	62.6(1.1)	52.0(1)	38.1(5)	152.7(1.7)	152.7	1.65
120	62.6(1.1)	52.0(1)	38.0 (5)	152.5(1.7)	152.6	1.65

Table 9. The parameters for approximation equations $X = p_0 + p_1 \times T \times 10^{-3}$, describing the temperature dependences of the unit-cell parameters of $Zn(NH_3)_2Cl_2$.

X	n	p_0	p_1	R^2
Based on single-crystal X-ray diffraction data (from −173 to 77 °C)				
a	1	7.7758(14)	0.461(14)	1.00000
b	1	8.08645(39)	0.4109(40)	1.00000
c	1	8.5055(23)	0.309(23)	1.00000
V	1	534.83(20)	78.0(2)	1.00000
Based on powder X-ray diffraction data (from 30 to 130 °C)				
a	1	7.77892(79)	0.4903(91)	1.00000
b	1	8.08340(76)	0.4226(88)	1.00000
c	1	8.50151(38)	0.3248(44)	1.00000
V	1	534.554(82)	82.73(96)	1.00000

3.6. Structural Complexity

The structural complexity values for $Zn(NH_3)_2Cl_2$, including all atoms (I_G, $I_{G,total}$) and excluding localized H-atoms ($I_{G(no\ H)}$, $I_{G,total(no\ H)}$), are provided in Table 10. The structural complexity per unit cell ($I_{G,total}$) is about three times higher when including H atoms.

Table 10. The structural complexity of $Zn(NH_3)_2Cl_2$, including all atoms (I_G, $I_{G,total}$) and without localized H-atoms ($I_{G(no\ H)}$, $I_{G,total(no\ H)}$).

	I_g, Bits/Atom	$I_{G,Total}$, Bits/Cell	$I_{G(no\ H)}$, Bits/Atom	$I_{G,Total(no\ H)}$, Bits/Cell
$Zn(NH_3)_2Cl_2$	2.187	48.107	1.522	15.219

4. Discussion

The crystal chemical studies demonstrate that anthropogenic $Zn(NH_3)_2Cl_2$ ("amminite") from the ChCB burned dump is completely identical to its synthetic analogue. Although phases from burned dumps under some circumstances could now be considered as valid mineral species [33], this zinc diammine chloride is definitely man-made (has anthropogenic or technogenic origin) due to the ad hoc introduction of the zinc plate. Thus, the possibility of the formation of $Zn(NH_3)_2Cl_2$ under completely natural conditions is still questionable.

In general, there are very few minerals containing ammine complexes (see Introduction). All these minerals contain copper and were found at the Pabellon de Pica guano deposit within the contact zone between bird guano and the surface of gabbro enriched with chalcopyrite, $CuFeS_2$. The latter, being exposed to air, oxidizes and serves as a source of Cu^{2+} for numerous supergene minerals [7–9]. From these five minerals, two are chlorides, and only ammineite, $CuCl_2(NH_3)_2$ (not to be confused with the anthropogenic "amminite" (Chesnokov et al.)), belongs to the class of diamminechlorides of the divalent metal cations with the general formula $M^{2+}(NH_3)_2Cl_2$ (see above), which also includes the studied $Zn(NH_3)_2Cl_2$. It is of interest that the crystal structures of $CuCl_2(NH_3)_2$ and $Zn(NH_3)_2Cl_2$ are not isotypic. In ammineite, $CuCl_2(NH_3)_2$, the coordination of Cu^{2+} is distorted octahedral, due to the Jahn–Teller effect, and the structure is based upon zigzag chains of distorted octahedra [6]. According to Bojar et al. [6], the formation of ammineite in nature was due to the reaction of Cu minerals with guano.

Natural zinc chlorides containing ammine complex (NH_3^0) or ammonium cation (NH^{4+}) are currently unknown. Only one zinc mineral with ammonium has been described, katerinopoulosite, $(NH_4)_2Zn(SO_4)_2 \cdot 6H_2O$, which was formed in the young oxidation zone of an ore enriched in sphalerite, ZnS, in Lavrion, Greece. The most probable source of ammonium was the leached soil saturated with organic residues [34]. On the other hand, hydrogen-free zinc chlorides and Cl-bearing Zn oxysalts

are only known to be in the oxidizing-type fumaroles of the Tolbachik volcano, Kamchatka, Russia: mellizinkalite, $K_3Zn_2Cl_7$ [35], flinteite, K_2ZnCl_4 [36], belousovite, $KZn(SO_4)Cl$ [37], chubarovite, $KZn_2(BO_3)Cl_2$ [38], cryobostryxite, $KZnCl_3{\cdot}2H_2O$ [39], prewittite, $KPb_{1.5}ZnCu_6O_2(SeO_3)_2Cl_{10}$ [40] and sofiite, $Zn_2(SeO_3)Cl_2$ [41]. Two natural hydrated zinc chlorides, simonkolleite, $Zn_5Cl_2(OH)_8{\cdot}H_2O$ [42], and cryobostryxite, $KZnCl_3{\cdot}2H_2O$ [39], are supergene minerals. Cryobostryxite forms as a product of the interaction of primary fumarolic Zn chlorides with atmospheric water or water vapor in the moderately hot (70–150 °C) zone of Tolbachik fumaroles, where ammonium minerals are also known, e.g., novograblenovite, $(NH_4)MgCl_3{\cdot}6H_2O$ [43]. However, in fumarolic systems, the formation of minerals containing ammine (NH_3^0) complexes seems hardly probable, since it requires the formation of Zn–N bonds.

Thus, although the question remains open, under certain geochemical conditions, the formation of $Zn(NH_3)_2Cl_2$ may occur in nature, for instance, in the environments that involve reactions of Zn-bearing minerals (for example, sphalerite-rich rocks) with complicated organic matter, such as guano which contains organic compounds with ammine groups. Apparently, the source of ammonia for the formation of $Zn(NH_3)_2Cl_2$ in the ChCB burned coal dumps was a special organic substance contained in coal-bearing dump material; however, we cannot say whether this is directly related to coal. This fact explains the difference in the number of compounds with ammonia (NH_3^0) and ammonium (NH^{4+}) described from the burned coal dumps of the ChCB: one species *vs* at least sixteen species, respectively. The presence of such special (specific) organic substances within the burning coal dumps of the ChCB is indirectly confirmed by the presence of other crystalline organic phases found there in sublimates of the "pseudofumaroles", such as $C_{10}H_{12}N_8O_8$ and kladnoite, $C_6H_4(CO)_2NH$ [2].

Upon heating, the $Zn(NH_3)_2Cl_2$ phase is stable up to about 150 °C. This is in good agreement with the data of Chesnokov and co-authors, who suggested temperatures of $Zn(NH_3)_2Cl_2$ formation lower than 200 °C [1]. The crystal structure of $Zn(NH_3)_2Cl_2$ expands anisotropically (Table 8, Figure 5); at the same time, the bond lengths within the ZnN_2Cl_2 tetrahedra practically do not change (within the errors; see Table S1 for details), which indicates that the thermal expansion of the structure is controlled by the changes in the hydrogen bonding system (most obviously fixed by the increase in the distance D...A, Table 5). The observed anisotropy is probably connected to a specific arrangement of hydrogen bonds relative to the crystallographic axes. Thus, the maximum expansion is observed along the *a* axis, while the largest relative increase in the distance D...A (3.549(3) Å at −173 °C and 3.634(4) at 77 °C) is observed for the bond N-H1A...Cl^2 (Table 6), which is oriented most closely to the *a* axis (Figures 5 and 6).

The role of H-bonds in the structural complexity values can be estimated as significant, using a calculation of I_G and $I_{G,total}$ including all atoms and without localized H-atoms ($I_{G(no\ H)}$, $I_{G,total(no\ H)}$) (Table 10). Thus, the $I_{G,total}/I_{G,total(no\ H)}$ value is 3.16, which is more than the similar value observed for halotrichite and related hydrates sulfates ($I_{G,total}/I_{G,total(no\ H)}$~2.33) [44]. At the same time, the structural complexity of $Zn(NH_3)_2Cl_2$ is relatively low, which is typical for halides: the average values of structural complexity for all minerals are estimated as I_G = 3.54(0.02) bits/atom and $I_{G,total}$ = 345(10) bits/cell, while, for halides, these values are I_G = 1.95(0.12) bits/atom and $I_{G,total}$ = 62.91(11.57) bits/cell [26].

5. Conclusions

(i). A detailed crystal chemical description of the anthropogenic $Zn(NH_3)_2Cl_2$ ("amminite") was carried out for the first time. It was found that this anthropogenic phase, formed under unique conditions of burned coal dumps, is identical to synthetic $Zn(NH_3)_2Cl_2$.

(ii). High-temperature powder and single crystals studies of the anthropogenic $Zn(NH_3)_2Cl_2$ are in a good agreement with each other and show that, upon heating, $Zn(NH_3)_2Cl_2$ is stable up to ca. 150 °C. This fact agrees well with the data on the temperature of its formation.

(iii). The Raman and IR spectroscopic characteristics of this phase are close to those reported for ammineite, $CuCl_2(NH_3)_2$, where the peaks corresponding to ammine (NH_3^0) groups are clearly distinguishable.
(iv). The thermal expansion of the anthropogenic mineral-like phase $Zn(NH_3)_2Cl_2$ is anisotropic and is determined by the system of hydrogen bonds. The geometrical parameters of the ZnN_2Cl_2 tetrahedra do not change upon heating.
(v). Apparently, the source of ammonia for the formation of $Zn(NH_3)_2Cl_2$ in the burned coal dumps of the ChCB was a special organic substance contained in the coal-bearing dump material. However, it is not known whether this is directly related to coal.
(vi). The formation of $Zn(NH_3)_2Cl_2$ in nature is possible under very specific conditions, such as in the interactions of zinc-bearing minerals with organic matter containing ammine (NH_3^0) groups (for example, with guano).
(vii). The structural complexity of $Zn(NH_3)_2Cl_2$ is relatively low. At the same time, the role of H-bonds in the values of the structural complexity of $Zn(NH_3)_2Cl_2$ can be estimated to be very significant.

Supplementary Materials: The following supporting information can be downloaded at: https://www.mdpi.com/article/10.3390/min13081109/s1, Figure S1: Powder X-ray diffraction patterns at different temperatures of $Zn(NH_3)_2Cl_2$. Table S1: Selected bond lengths (Å) and angles (°) of $Zn(NH_3)_2Cl_2$ at different temperatures. Table S2: The comparison of the main Raman bands for $Zn(NH_3)_2Cl_2$ and ammineite, $CuCl_2(NH_3)_2$. CIF: Crystallographic Information file (CIF) for the crystal structure of $Zn(NH_3)_2Cl_2$ at −73 °C.

Author Contributions: Conceptualization, A.A.Z. (Andrey A. Zolotarev), M.S.A., R.M.S. and S.V.K.; methodology, A.A.Z. (Andrey A. Zolotarev), M.S.A., A.A.Z. (Anatoly A. Zolotarev) and I.V.P.; formal analysis, M.A.R.; investigation, R.M.S., M.S.A., A.A.Z. (Andrey A. Zolotarev), M.G.K., N.S.V. and V.N.B.; writing—original draft preparation, A.A.Z. (Andrey A. Zolotarev); writing—review and editing, M.S.A., I.V.P., M.G.K., V.N.B., S.V.K., R.M.S., A.A.Z. (Anatoly A. Zolotarev), N.S.V. and M.A.R.; visualization, A.A.Z. (Andrey A. Zolotarev), M.S.A. and R.M.S.; supervision A.A.Z. (Andrey A. Zolotarev) and S.V.K. All authors have read and agreed to the published version of the manuscript.

Funding: This research was funded by the Russian Science Foundation, grant number 23-27-00147, https://rscf.ru/en/project/23-27-00147/ (accessed on 10 July 2023).

Data Availability Statement: Not applicable.

Acknowledgments: The X-ray diffraction studies were performed in the X-ray Diffraction Resource Centre of St. Petersburg State University. The chemical analytical and spectroscopic studies were performed in the "Geomodel" Resource Centre of St. Petersburg State University.

Conflicts of Interest: The authors declare no conflict of interest.

References

1. Chesnokov, B.V.; Bazhenova, L.F.; Bushmakin, A.F.; Vilisov, V.A.; Lotova, E.V.; Michal, T.A.; Nishanbaev, T.P.; Shcherbakova, E.P. New minerals of burned spoil-heaps of the Chelyabinsk coal basin (Communication No. 2). In *New Data on the Mineralogy of Endogenous Deposits and Technogenesis Zones of the Urals*; Ural Branch of RAS: Sverdlovsk, Russia, 1991; pp. 3–36. (In Russian)
2. Chesnokov, B.V.; Shcherbakova, E.P.; Nishanbaev, T.P. *Minerals of Burnt Dumps of the Chelyabinsk Coal Basin*; Ural Branch of RAS: Miass, Russia, 2008; pp. 1–139. (In Russian)
3. Parafiniuk, J.; Kruszewski, Ł. Ammonium minerals from burning coal-dumps of the Upper Silesian Coal Basin (Poland). *Geol. Quart.* **2009**, *53*, 341–356.
4. Zolotarev, A.A.; Zhitova, E.S.; Krzhizhanovskaya, M.G.; Rassomakhin, M.A.; Shilovskikh, V.V.; Krivovichev, S.V. Crystal Chemistry and High-Temperature Behaviour of Ammonium Phases NH_4MgCl_3·6H2O and $(NH_4)_2Fe^{3+}Cl_5·H_2O$ from the Burned Dumps of the Chelyabinsk Coal Basin. *Minerals* **2019**, *9*, 486. [CrossRef]
5. Zhitova, E.S.; Sergeeva, A.V.; Nuzhdaev, A.A.; Krzhizhanovskaya, M.G.; Chubarov, V.M. Tschermigite from thermal fields of Southern Kamchatka: High-temperature transformation and peculiarities of IR-spectrum. *Zapiski RMO (Proc. Russian Mineral. Soc.)* **2019**, *148*, 100–116. (In Russian)
6. Bojar, H.P.; Walter, F.; Baumgartner, J.; Färber, G. Ammineite, $CuCl_2(NH_3)_2$, a new species containing an ammine complex: Mineral data and crystal structure. *Can. Mineral.* **2010**, *48*, 1359–1371. [CrossRef]

7. Chukanov, N.V.; Zubkova, N.V.; Mohn, G.; Pekov, I.V.; Pushcharovsky, D.Y.; Zadov, A.E. Chanabayaite, $Cu_2Cl(N_3C_2H_2)_2(NH_3,Cl,H_2O,\square)_4$, a new mineral containing triazolate anion. *Zapiski RMO (Proc. Russian Mineral. Soc.)* **2015**, *144*, 36–47. (In Russian)
8. Chukanov, N.V.; Zubkova, N.V.; Möhn, G.; Pekov, I.V.; Belakovskiy, D.I.; Van, K.V.; Britvin, S.N.; Pushcharovsky, D.Y. Triazolite, $NaCu_2(N_3C_2H_2)_2(NH_3)_2Cl_3 \cdot 4H_2O$, a new mineral species containing 1,2,4-triazolate anion, from a guano deposit at Pabellón de Pica, Iquique Province, Chile. *Mineral. Mag.* **2018**, *82*, 1007–1014. [CrossRef]
9. Chukanov, N.V.; Britvin, S.N.; Möhn, G.; Pekov, I.V.; Zubkova, N.V.; Nestola, F.; Kasatkin, A.V.; Dini, M. Shilovite, natural copper (II) tetrammine nitrate, a new mineral species. *Mineral. Mag.* **2015**, *79*, 613–623. [CrossRef]
10. Bojar, H.; Walter, F.; Baumgartner, J. Joanneumite, $Cu(C_3N_3O_3H_2)_2(NH_3)_2$, a new mineral from Pabellón de Pica, Chile and the crystal structure of its synthetic analogue. *Mineral. Mag.* **2017**, *81*, 155–166. [CrossRef]
11. Von Zelewsky, A. *Stereochemistry of Coordination Compounds*; Wiley: Chichester, UK, 1996; pp. 1–266.
12. Lippard, S.J.; Berg, J.M. *Principles of Bioinorganic Chemistry*; University Science Books: Mill Valley, CA, USA, 1994; pp. 1–411.
13. Christensen, C.H.; Sørensen, R.Z.; Johannessen, T.; Quaade, U.J.; Honkala, K.; Elmøe, T.D.; Køhler, R.; Nørskov, J.K. Metal ammine complexes for hydrogen storage. *J. Mater. Chem.* **2005**, *15*, 4106–4108. [CrossRef]
14. Ivšić, T.; Bi, D.W.; Magrez, A. New refinement of the crystal structure of $Zn(NH_3)_2Cl_2$ at 100 K. *Acta Crystallogr. E Crystallogr. Commun.* **2019**, *75*, 1386–1388. [CrossRef]
15. Gardner, P.J.; Pang, P.; Preston, S. Thermodynamics of the dissociation of $ZnCl_2(NH_3)_2$ by modified entrainment. *Thermochim. Acta* **1989**, *138*, 371–374. [CrossRef]
16. Bubnova, R.S.; Firsova, V.A.; Filatov, S.K. Software for determining the thermal expansion tensor and the graphic representation of its characteristic surface (Theta to Tensor-TTT). *Glass Phys. Chem.* **2013**, *39*, 347–350. [CrossRef]
17. *CRYSALISPRO Software System*; Version 1.171.39.44; Rigaku Oxford Diffraction: Oxford, UK, 2015.
18. Sheldrick, G.M. Crystal structure refinement with SHELXL. *Acta Crystallogr. Struct. Chem.* **2015**, *71*, 3–8. [CrossRef]
19. Dolomanov, O.V.; Bourhis, L.J.; Gildea, R.J.; Howard, J.A.K.; Puschmann, H. OLEX2: A complete structure solution, refinement and analisis program. *Appl. Crystallogr.* **2009**, *42*, 339–341. [CrossRef]
20. Momma, K.; Izumi, F. VESTA 3 for three-dimensional visualization of crystal, volumetric and morphology data. *J. Appl. Crystallogr.* **2011**, *44*, 1272–1276. [CrossRef]
21. Schuck, G.; Iwata, A.; Sasaki, A.; Himeda, A.; Konaka, H.; Muroyama, N. PDXL structure analysis wizard. *Acta Crystallogr. A Found. Crystallogr.* **2011**, *A67*, C799–C800. [CrossRef]
22. *BRUKER-AXS Topas V4.2 General Profile and Structure Analysis Software for Powder Diffraction Data*; Bruker-AXS: Karlsruhe, Germany, 2009.
23. Blatov, V.A.; Shevchenko, A.P.; Proserpio, D.M. Applied topological analysis of crystal structures with the program package ToposPro. *Cryst. Growth Des.* **2014**, *14*, 3576–3586. [CrossRef]
24. Yamaguchi, T.; Lindqvist, O. The Crystal Structure of Diamminedichlorozinc(II), $ZnCl_2(NH_3)_2$. A New Refinement. *Acta Chem. Scand.* **1981**, *35*, 727–728. [CrossRef]
25. Krivovichev, S.V. Structural complexity of minerals: Information storage and processing in the mineral world. *Mineral. Mag.* **2013**, *77*, 275–326. [CrossRef]
26. Krivovichev, S.V.; Krivovichev, V.G.; Hazen, R.M.; Aksenov, S.M.; Avdontceva, M.S.; Banaru, A.M.; Gorelova, L.A.; Ismagilova, R.M.; Kornyakov, I.V.; Kuporev, I.V.; et al. Structural and Chemical Complexity of Minerals: An Update. *Mineral. Mag.* **2022**, *86*, 183–204. [CrossRef]
27. Košek, F.; Němec, I.; Jehlička, J. Raman study of several Cu-bearing minerals from the guano deposit at Pabellón de Pica, Tarapaca region, Chile. *J. Raman Spectrosc.* **2023**, *1*, 1–11. [CrossRef]
28. Hall, J.R.; Hirons, D.A. Infrared and Raman spectra of Magnus' Green salt, $[Pt(NH_3)_4]$ $[PtCl_4]$, and its Deuterate. *Inorg. Chim. Acta* **1979**, *34*, L277–L279. [CrossRef]
29. Frezotti, T.; Tecce, F.; Casagli, A. Raman spectroscopy for fluid inclusion analysis. *J. Geochem. Explor.* **2012**, *112*, 1–20. [CrossRef]
30. Chukanov, N.V. *Infrared Spectra of Mineral Species: Extended Library*; Springer: Dordrecht, The Netherlands, 2014; 1726p.
31. Wang, C.; Zhan, H.; Lu, X.; Jing, R.; Zhang, H.; Yang, L.; Li, X.; Yue, F.; Zhou, D.; Xia, Q. A recyclable cobalt(iii)–ammonia complex catalyst for catalytic epoxidation of olefins with air as the oxidant. *New J. Chem.* **2021**, *45*, 2147–2156. [CrossRef]
32. MacGillavry, C.H.; Bijvoet, J.M.Z. Die Kristallstruktur von $Zn(NH_3)_2Cl_2$ und $Zn(NH_3)_2Br_2$. *Z. Kristallogr.* **1936**, *94*, 249–255. [CrossRef]
33. Parafiniuk, J.; Hatert, F. New IMA CNMNC guidelines on combustion products from burning coal dumps. *Eur. J. Mineral.* **2020**, *32*, 215–217. [CrossRef]
34. Chukanov, N.V.; Pekov, I.V.; Belakovskiy, D.I.; Britvin, S.N.; Stergiou, V.; Voudouris, P.; Magganas, A. Katerinopoulosite, $(NH_4)_2Zn(SO_4)_2 \cdot 6H_2O$, a new mineral from the Esperanza mine, Lavrion, Greece. *Eur. J. Mineral.* **2018**, *30*, 821–826. [CrossRef]
35. Pekov, I.V.; Zubkova, N.V.; Yapaskurt, V.O.; Lykova, I.S.; Belakovskiy, D.I.; Vigasina, M.F.; Sidorov, E.G.; Britvin, S.N.; Pushcharovsky, D.Y. New zinc and potassium chlorides from fumaroles of the Tolbachik volcano, Kamchatka, Russia: Mineral data and crystal chemistry. I. Mellizinkalite, $K_3Zn_2Cl_7$. *Eur. J. Mineral.* **2015**, *27*, 247–253. [CrossRef]
36. Pekov, I.V.; Zubkova, N.V.; Yapaskurt, V.O.; Britvin, S.N.; Vigasina, M.F.; Sidorov, E.G.; Pushcharovsky, D.Y. New zinc and potassium chlorides from fumaroles of the Tolbachik volcano, Kamchatka, Russia: Mineral data and crystal chemistry. II. Flinteite, K_2ZnCl_4. *Eur. J. Mineral.* **2015**, *27*, 581–588. [CrossRef]

37. Siidra, O.I.; Nazarchuk, E.V.; Lukina, E.A.; Zaitsev, A.N.; Shilovskikh, V.V. Belousovite, $KZn(SO_4)Cl$, a new sulfate mineral from the Tolbachik volcano with apophyllite sheet-topology. *Mineral. Mag.* **2018**, *82*, 1079–1088. [CrossRef]
38. Pekov, I.V.; Zubkova, N.V.; Pautov, L.A.; Yapaskurt, V.O.; Chukanov, N.V.; Lykova, I.S.; Britvin, S.N.; Sidorov, E.G.; Pushcharovsky, D.Y. Chubarovite, $KZn_2(BO_3)Cl_2$, a new mineral species from the Tolbachik volcano, Kamchatka, Russia. *Can. Mineral.* **2015**, *53*, 273–284. [CrossRef]
39. Pekov, I.V.; Zubkova, N.V.; Britvin, S.N.; Yapaskurt, V.O.; Chukanov, N.V.; Lykova, I.S.; Sidorov, E.G.; Pushcharovsky, D.Y. New zinc and potassium chlorides from fumaroles of the Tolbachik volcano, Kamchatka, Russia: Mineral data and crystal chemistry. III. Cryobostryxite, $KZnCl_3 \cdot 2H_2O$. *Eur. J. Mineral.* **2015**, *27*, 805–812. [CrossRef]
40. Shuvalov, R.R.; Vergasova, L.P.; Semenova, T.F.; Filatov, S.K.; Krivovichev, S.V.; Siidra, O.I.; Rudashevsky, N.S. Prewittite, $KPb_{1.5}Cu_6Zn(SeO_3)_2O_2Cl_{10}$, a new mineral from Tolbachik fumaroles, Kamchatka peninsula, Russia: Description and crystal structure. *Am. Mineral.* **2013**, *98*, 463–469. [CrossRef]
41. Vergasova, L.P.; Filatov, S.K.; Semenova, T.F.; Filosofova, T.M. Sofiite $Zn_2(SeO_3)Cl_2$—A new mineral from volcanic sublimates. *Zapiski RMO (Proc. Russian Mineral. Soc.)* **1989**, *118*, 65–69. (In Russian)
42. Schmetzer, K.; Schnorrer-Köhler, G.; Medenbach, O. Wülfingite, epsilon-$Zn(OH)_2$, and simonkolleite, $Zn_5(OH)_8Cl_2 \cdot H_2O$, two new minerals from Richelsdorf, Hesse, FRG. *Neues Jahrb. Mineral. Monatshefte* **1985**, *151*, 145–154.
43. Okrugin, V.M.; Kudaeva, S.S.; Karimova, O.V.; Yakubovich, O.V.; Belakovskiy, D.I.; Chukanov, N.V.; Zolotarev, A.A.; Gurzhiy, V.V.; Zinovieva, N.G.; Shiryaev, A.A.; et al. The new mineral novograblenovite, $(NH_4,K)MgCl_3 \cdot 6H_2O$ from the Tolbachik volcano, Kamchatka, Russia: Mineral description and crystal structure. *Mineral. Mag.* **2019**, *83*, 223–231. [CrossRef]
44. Zhitova, E.S.; Sheveleva, R.M.; Zolotarev, A.A.; Krivovichev, S.V.; Shilovskikh, V.V.; Nuzhdaev, A.A.; Nazarova, M.A. The crystal structure of magnesian halotrichite, $(Fe,Mg)Al_2(SO_4)_4 \cdot 22H_2O$: Hydrogen bonding, geometrical parameters and structural complexity. *J. Geosci.* **2023**, *68*, 111–134. [CrossRef]